AXIAL FLOW REVERSAL AND ITS SIGNIFICANCE IN AIR-SPARGED HYDROCYCLONE (ASH) FLOTATION

J.D. MILLER, A. DAS and D. YIN
Pittsburgh Coal Conference
Department of Metallurgical Engineering
University of Utah
Salt Lake City, UT 84112, U.S.A.

ABSTRACT

In recent years the potential of air-sparged hydrocyclone (ASH) flotation for fine coal cleaning has been demonstrated both in pilot plant testing and in a plant-site demonstration program. Further improvements in the ASH technology will depend, to some extent, on improved understanding of the complex multiphase fluid flow.

Froth transport plays a very important role in determining the efficiency of fine coal cleaning by ASH flotation. It should be noted that the surface of zero axial velocity is of particular significance in froth transport because the location of this surface actually accounts for the amount of froth being transported to the overflow. In this regard, the axial flow reversal has been examined based on specially designed tracer experiments. On the basis of these experimental results, modeling efforts were made to characterize the flow pattern in the ASH. The theoretical predictions based on turbulent fluid dynamic considerations were found to describe experimental observations regarding the surface of zero axial velocity. These results that define the surface of zero axial velocity together with froth phase features established from x-ray CT measurements provide an excellent description of the flow characteristics in ASH flotation and explain the effect of various process variables, such as dimensionless area (A*), dimensionless flowrate (Q*), inlet pressure, percent solids, etc., on flotation recovery. On this basis it is expected that further advances in the design and operation of the ASH system can be made, leading to more efficient use of the ASH technology for fine coal cleaning.

INTRODUCTION

The high specific capacity air sparged hydrocyclone (ASH) has been developed for fine particle flotation in a centrifugal force field. Typically, the ASH has specific capacity 100 times that of conventional flotation machines or columns. The general fundamental of air sparged hydrocyclone flotation and its applications have been described in the literature on numerous occasions [1-6]. It's use for fine coal cleaning is particularly noteworthy [7-9.]. Only recently has the effect of fluid flow characteristics on ASH flotation been examined in detail [10, 11].

By way of review, the suspension enters the ASH through a tangential inlet at the top and exits through an annular underflow opening at the bottom in swirl flow as indicated in Figure 1. In the absence of the froth pedestal at the bottom, all of the swirl flow would exit through the bottom of the ASH. However, the tapered froth pedestal prevents all of the flow from exiting through the underflow opening at the bottom and causes some of the multiphase flow to have an upward motion. Therefore, some of the flow (ideally froth and hydrophobic particles) exits through the overflow opening (the vortex finder finder pipe) at the top. As in a conventional hydrocyclone, it is expected that at any axial location there will be a point at some radial position where the axial velocity is zero [12, 13]. In the region between this surface and the air core interface, flow will be upward towards the vortex finder whereas in the region between this surface andthe porous tube, flow will be downward towards the underflow opening. On this basis, a surface of zero axial velocity (ZAV) can be defined for the ASH. A change in the operating conditions is expected to change the spatial coordinates (location) of this surface and thus cause a change in the transport characteristics of the ASH leading to a change in the recovery of the overflow product. Measurements were undertaken to determine the location of this surface of ZAV for various operating conditions in order to characterize the performance of the ASH with regard to its transport properties. Experiments were carried out during quartz flotation with amine to locate the ZAV surface by using a lithium chloride solution for analysis technique and the results analyzed together with radial density profiles, as determined by x-ray CT, in order to explain the observed flotation response.

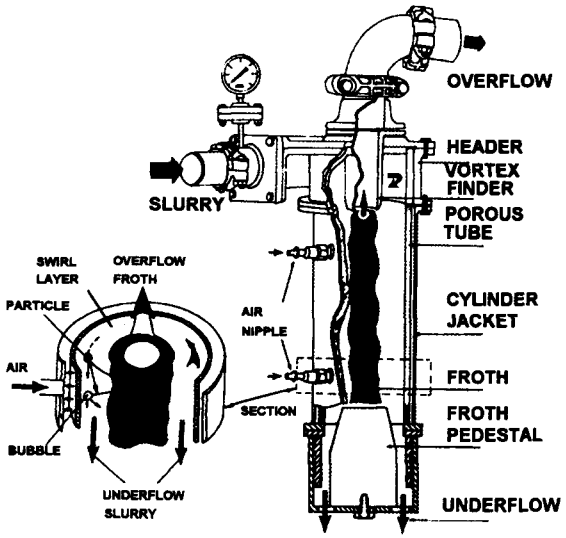

Fig. 1. Perspective of the air-sparged hydrocyclone.

EXPERIMENTAL PROCEDURE

Seven almost equally spaced small holes were drilled in the porous tube section (305 mm in length) of the ASH at different axial positions. These sampling ports were sealed from inside and outside with silicone glue. Needles were then inserted through these holes. The silicone provided for easy movement of the needles while preventing any leakage at the same time. Thus, through any axial port, it was possible to inject the lithium chloride tracer solution at any radial position inside the ASH by moving the needle a prescribed distance in the radial direction.

From x-ray CT data the air core diameters for various experimental conditions were known *a priori* as well as the combined spatial extent of the froth phase and swirl layer. Depending upon these dimensions, tracer solution was injected at different radial positions in the region between air core interface and the porous tube surface. During quartz flotation at steady state, the tracer solution (5 cc) was injected for different radial locations at each axial position and the product streams were sampled simultaneously. It was anticipated that at any axial position, if the tracer solution was injected at the porous tube side of the ZAV surface, most of the lithium chloride solution would report to the underflow stream. On the other hand, if the tracer solution was injected at the air core side of the ZAV surface, the overflow stream would have a high concentration of lithium chloride solution. In this way, based on the partition of the tracer between the product streams, the ZAV surface was determined [14].

RESULTS AND DISCUSSION

Using the technique described above, the influence of the following operating variables on the position of the ZAV surface was studied: A*- the ratio of overflow opening area to underflow opening area; Q*- the ratio of air flow rate to slurry flow rate; Φ - percent solids in the feed suspension; P - slurry inlet pressure. These results are presented and discussed in the following sections.

Dimensionless Area (A*)

Figure 2 compares the ZAV surface for two different A* values with Q* = 4.55, 5% solids in feed, and inlet pressure of 10.5 psi. It can be seen that as A* is increased from 0.74 to 1.00, the ZAV surface shifts outward toward the porous tube. Although not substantially large, this shift corresponds to a large amount of froth being carried to the overflow for the higher A* value (A*=1.00) and thus accounts for the higher recovery found in the flotation experiments. See Figure 3. Interestingly, the ZAV surface intersects the radial density profiles at different points in the two cases. It can be seen clearly from Figure 3 that, because of the location of the ZAV surface, almost all the froth is being carried to the overflow for A* = 1.00. In this case the ZAV surface does not intersect the froth phase at any axial location. Thus, there is no loss of froth to the underflow and the recovery in this case is 97.2%. On the other hand, since the ZAV surface intersects the froth phase at almost all axial locations for A* = 0.74, a lot of froth is expected to be carried to the underflow. This has indeed been observed as the recovery to the overflow is 15.5% in this case.

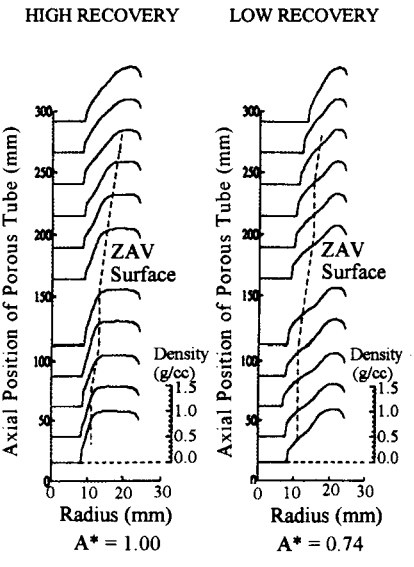

Fig. 2. The ZAV surface superimposed on the radial density profiles at two different A* values with Q* = 4.55 and 10.5 psi inlet pressure for 15% solids in the feed.

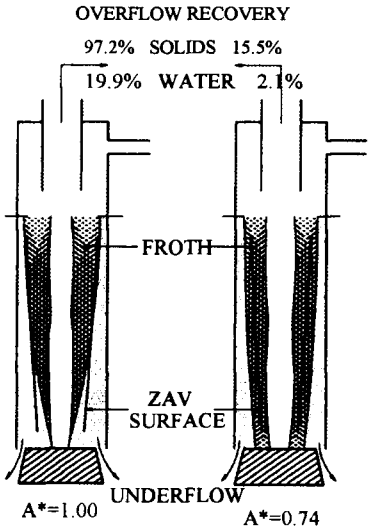

Fig. 3. Axial view of the flow regimes with the ZAV surface at two different A* values with Q*=4.55 and 10.5 psi inlet pressure for 15% solids in the feed.

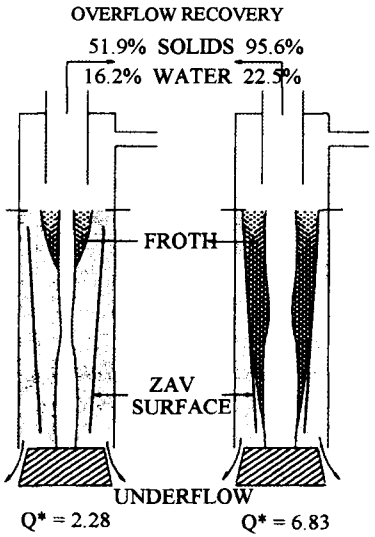

Fig. 4. Axial view of the flow regimes with the ZAV surface at two different Q* values with A*=1.00 and 10.5 psi inlet pressure for 15% solids in the feed.

Dimensionless Flow Rate (Q*)

It was found that Q* has no noticeable impact on the ZAV surface. The surface was found to have the same location independent of Q*. Thus, the axial flow reversal characteristics that determine froth transport are not a function of Q*. Nevertheless, a lower recovery was observed with a lower Q* (Q* = 2.28) than with a higher Q* (Q* = 6.83). Insufficient air flow prevents the formation of a stable froth and causes the recovery to drop, the axial flow reversal characteristics being comparable in the two cases. In other words, had there been enough froth with Q* = 2.28, it would have been carried to the overflow, resulting in good recovery. The axial views of the flow regimes along with the ZAV surface for the above two cases are shown in Figure 4. It can be seen from this figure that in both the cases the ZAV surface does not intersect the froth phase. At a low Q* (Q* = 2.28) the froth phase is not stabilized due to insufficient air flow. The hydrophobic particles remained centrifuged at the wall and were eventually carried to the underflow resulting in a poor recovery. On the other hand, the froth phase is stabilized at a high Q* (Q* = 6.83), and is readily carried to the overflow giving good recovery.

Percent Solids (Φ)

As was found in the case of Q* the ZAV surface does not change significantly with an high recovery shown in Figure 3 was not affected by a change in solids concentration when A* was kept at 1.00. This implies that froth transport is favorable under these conditions. The axial views of the flow regimes and the ZAV surface for two different solids concentrations are shown in Figure 5. It can be seen from this figure that in both cases all

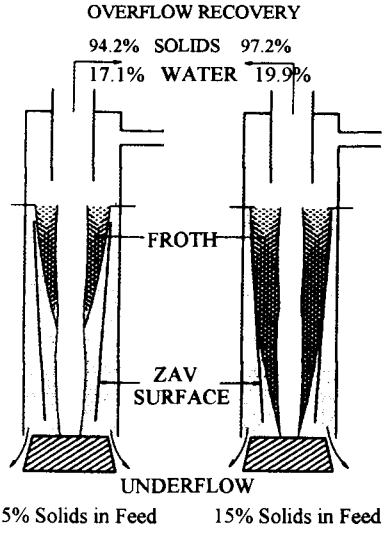

Fig. 5. Axial view of the flow regimes with the ZAV surface at two different solids concentrations with A* =1.00, Q* = 4.55 and 10.5 psi inlet pressure.

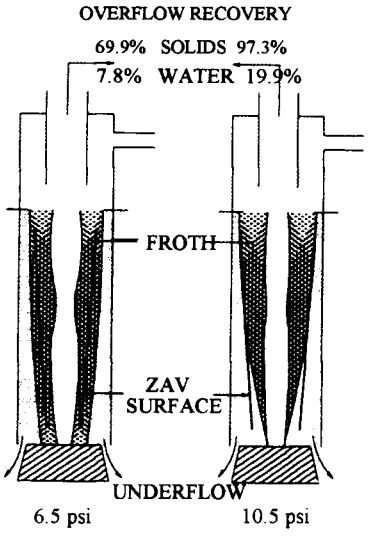

Fig. 6. Axial view of the flow regimes with the ZAV surface at two different inlet pressure with A* = 1.00, Q* = 4.55 and 15% solids in the feed.

the froth is transported to the overflow since the ZAV surface does not intersect the froth phase in either case. In fact, more that 94% recovery was observed in both cases.

Inlet Pressure

The inlet pressure at which the slurry is being fed to the ASH is expected to change the flow characteristics of the ASH as the entire velocity distribution is dependent on the inlet velocity and hence inlet pressure. However, the ZAV surface increase in solids concentration at A*=1.00. In this regard, it should be noted that the shifts only a little towards the porous tube wall as the inlet pressure is increased from 6.5 psi to 10.5 psi. Consequently, the amount of froth being carried to the overflow is more in the case of 10.5 psi and this explains the observation that the recovery is greater at 10.5 psi than at 6.5 psi as shown in Figure 6. It can be seen from this figure that because of the location of the ZAV surface, some froth is being carried to the underflow at a low inlet pressure (6.5 psi) giving lower recovery while all the froth is carried to the overflow at a high inlet pressure (10.5 psi) resulting in a high recovery of 97.3%. Therefore, with respect to the inlet pressure variable it appears that froth transport to the overflow can limit flotation recovery under certain circumstances..

FLOW SIMULATION BY COMPUTATIONAL FLUID DYNAMICS (CFD)

On the basis of these experimental results, modeling efforts were made to characterize the flow pattern in the ASH [15]. The Navier-Stokes equations together with an appropriate continuity equation were transformed and cast into three equations involving vorticity, stream function and angular momentum. With such an approach, the theoretical prediction based on

turbulent fluid dynamic considerations was found to describe experimental observations regarding the ZAV surface. Calculations were carried out for different A* values while the other conditions were held constant. Figure 7 shows the influence of A* on the position of the ZAV surface as measured and as predicted by CFD. First, it can be seen from this figure that all lines show a similar trend: the ZAV surfaces have a slight slope towards the center from the top to the bottom of the ASH. Near the pedestal, the ZAV surface suddenly shifts towards the wall. The slopes do not change significantly with an increase in A*. Another trend that can be observed is that the ZAV surfaces move outward with an increase in A*. This indicates that the up-flow region expands with an increase in A* and more fluid will report to the overflow under such conditions, a finding which is consistent with what has been observed in practice. Of cause, as is evident from Figure 7, the predicted surfaces are more vertical than the measured ones. The difference is due to the fact that a vertical cylindrical air core interface was used as an approximation for the boundary condition in order to reduce the calculation complexity. The predicted surface of ZAV will be improved if the actual air core interface were used for the boundary condition

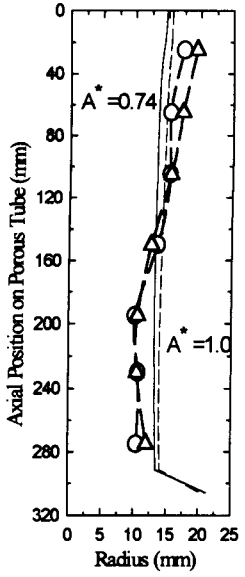

Fig. 7. Comparison of predicted and measured locations of the ZAV surface.

SUMMARY AND CONCLUSION

A study of the location of the surface of zero axial velocity (ZAV) was carried out. The location of the ZAV surface is critical for efficient froth transport and recovery by ASH flotation. If this surface coincides with the froth phase-swirl layer interface, best results will be obtained. However, depending upon the conditions, this surface may intersect the froth phase and under these circumstances a portion of the froth is lost to the underflow, causing the recovery to drop.

It was found that as the value of A* is increased, thefroth phase shrinks towards the center of the ASH, the ZAV surface shifts a little bit outward and more froth is carried to the overflow. Consequently, the recovery increases.

The ZAV surface also shifts towards the porous tube wall with an increase in inlet pressure causing a larger amount of froth to be transported to the overflow. Therefore, an increased recovery was observed at higher inlet pressures up to some limit depending on particle mass.

Unlike A* and inlet pressure, it appears that Q* and percent solids in the feed slurry do not have any noticeable impact on the location of the ZAV surface.

Acknowledgments

The financial support from the Department of Energy, Grant No.DE-FG2290PC90311 and the National Science Foundation, Grant No. CTS9000406 are gratefully acknowledged

References

1. J.D. Miller, The Concept of an Air-Sparged Hydrocyclone. 110 AIME Annual Meeting, Chicago, (1981) 1-10.
2. J.D. Miller and D.J. Kinneberg, Fast Flotation with an Air-Sparged Hydrocyclone. Proceedings of MINTEK 50, Johannesburg, South Africa, (1984) 373.
3. J.D. Miller, K.R. Upadrashta, D.J. Kinneberg, D.J. and S. Gopalakrishnan, Fluid-Flow Phenomena in the Air-Sparged Hydrocyclone. Proceedings of XV IMPC, Cannes, France, 2 (1985) 87-99.
4. J.D. Miller, Y. Ye, E. Pacquet, M.W. Baker and S. Gopalakrishnan, Design and Operating Variables in Flotation Separations with the Air-Sparged Hydrocyclone, Proceedings of XVI IMPC, Stockholm, Sweden, Elsevieer, Amsterdam, (1988) 499-510.
5. Y. Ye, S. Gopalakrishnan, E. Pacquet and J.D. Miller, Development of the Air-Sparged Hydrocyclone --- A Swirl Flotation Column. Column Flotation 1988, SME/AIME, (1988) 305-313.
6. J.D Miller and Y. Ye, Froth Characteristics in Air-Sparged Hydrocyclone Flotation, Mineral Processing and Extractive Metallurgy Review, 5 (1989) 307-329.
7. J.D. Miller and M.C. Van Camp, Fine Coal Flotation in a Centrifugal Field with an Air-Sparged Hydrocyclone, Mining Engineering, SME/AIME, (1982) 1575.
8. J.D Miller, Y. Ye, M.W. Baker and E. Pacquet, The Air-Sparged Hydrocyclone for Fine Coal Flotation. Proceedings of MINExpo International 88., American Mining Congress, (1988) 1:1.
9. J.D. Miller, Y. Ye and S. Gopalakrishnan, Testing of Large-Diameter Air-Sparged Hydrocyclones for Fine Coal Flotation at the Homer City Coal Preparation Plant, Coal Preparation 92, 9th International Coal Preparation Exhibition and Conference, Cincinnati, Ohio, (1992) 349-366.
10. J.D. Miller and A. Das, Swirl Flow Characteristics and Froth Phase Features in Air-Sparged Hydrocyclone Flotation as Revealed by X-Ray CT Analysis. International Journal of Mineral Processing, to be published.
11. J.D. Miller and A. Das, Flow Phenomena and its Impact on Air-Sparged Hydrocyclone Flotation of Quartz. Minerals and Metallurgical Processing, SME, 1994.
    D.F. Kesall, A Study of the Motion of Solid Particles in a Hydraulic Cyclone. Trans.
12. Inst. Chem. Engr. 30 (1952) 87-109.
    D. Bradley, The Hydrocyclone, Pergamon Press, New York, 1965.
13. A. Das, Characterization of Multiphase Flow During Air-Sparged Hydrocyclone
14. Flotation of Quartz as Revealed by X-Ray Computed Tomography, Ph.D. Thesis, University of Utah, 1994.
15. D. Yin, Q. Yu and J.D. Miller, Numerical Simulation of Fluid Motion in the Air-Sparged Hydrocyclone, to be published.